

Elastic properties of thin sandwich panels with fibrous metallic cores

A.E. Markaki and T.W. Clyne

Department of Materials Science & Metallurgy, Cambridge University, Pembroke Street
Cambridge CB2 3QZ, UK

Abstract

A sandwich material, based on a pair of thin stainless steel faceplates separated by a core incorporating stainless steel fibres, has recently been developed. This material has the potential to exhibit an attractive combination of properties, while retaining formability and general handling characteristics similar to those of conventional steel sheet. Two different core structures have been investigated: (a) transversely-aligned fibres bonded to the faceplates by adhesive and (b) a 3-dimensional network of fibres brazed to each other, and also to the faceplates. The beam stiffnesses of these sheets, and also their through-thickness Young's moduli, have been measured and compared with theoretical predictions.

Introduction

It has long been recognised that sandwich structures, composed of stiff outer layers held apart by a low density core, offer the potential for very high specific stiffness and other attractive mechanical properties. Most such structures are created by an assembly step of some sort, before or during component manufacture. This limits the flexibility of the production process and is relatively expensive. Nevertheless, there is considerable current interest in sandwich structures of different types, many of them based on metallic faceplates and having metal-containing cores - often made of stochastic cellular metals[1-3] or some more regular structure such as a truss assembly[4-6]. However, traditional approaches to the fabrication of the latter (eg investment casting) are cumbersome and economically unattractive. A particular case of cellular metals is those made of a metallic fibre network of some sort. A novel type of a sandwich steel sheet with a fibrous stainless steel core has recently been developed[7] based on a pair of thin ($\sim 200 \mu\text{m}$) stainless steel faceplates. This material has been termed a Hybrid Stainless Steel Assembly (HSSA). It can in principle offer a highly attractive set of property combinations, such as low areal density, high beam stiffness, efficient energy absorption during crushing and good vibrational damping capacity. Furthermore, the overall thickness of the sheet ($\sim 1 \text{ mm}$), and certain features of the core structure, are such that its processing characteristics can be comparable with those of a conventional monolithic metallic sheet. Some work has recently been published on the elastic properties[8] and interfacial delamination behaviour[9] of such material.

In the present paper, a study is presented of the beam stiffness and through-thickness Young's modulus of two different variants of HSSA material. Experimental data are correlated with predictions based on simple analytical treatments.

Experimental Procedures

Material Production

Two core structures have been investigated: (a) transversely-aligned fibres bonded to the faceplates by adhesive (designated "flocked sheet") and (b) 3-dimensional brazed fibre array brazed to the faceplates ("short fibre 3-D array sheet"). In both materials, the faceplates were $200 \mu\text{m}$ thick 316L stainless steel. Manufacturing procedures are briefly outlined below:

(a) Flocked sheet. This is made by a flocking process[7], in which short ($\sim 1 \text{ mm}$) drawn 316L stainless steel fibres, about $25 \mu\text{m}$ in diameter, are approximately transversely aligned - see Fig.1(a). The fibre volume fraction in the core is about 8%.

(b) Short fibre 3-D array. This consists of a 3-D network of fibres bonded to each other, and also to the faceplates, using a nickel-based braze alloy - see Fig.1(b). The fibres are inclined at various angles to the vertical, with an average value of the order of 60° . They occupy about 10% of the volume of the core and are made of 446 (ferritic) stainless steel, melt extracted to lengths of 2.5 mm.

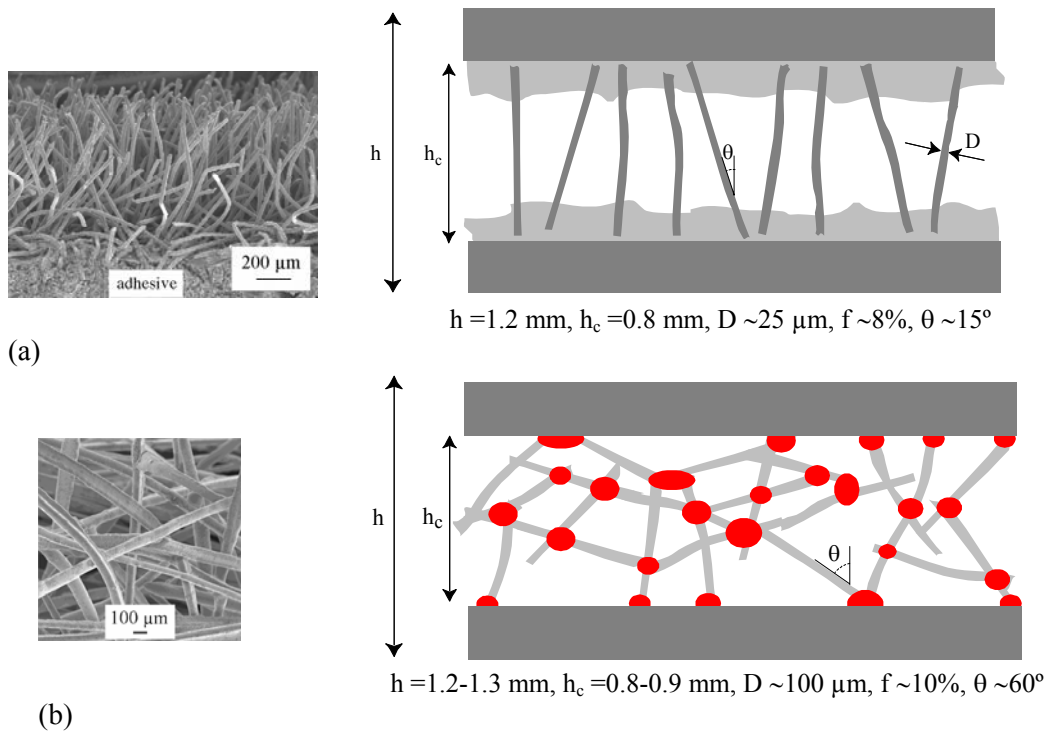


Fig.1: SEM micrographs, showing cross-sectional views of the cores, and schematic depictions of the structure of (a) flocked sheet and (b) short fibre 3-D array sheet.

Beam stiffness

Fig. 2 shows predicted and measured beam stiffnesses, plotted against the areal density. Fig.2(a) compares plots for solid steel, titanium and aluminium sheets with that for a sandwich composed of 200 μm steel faceplates and an isotropic epoxy core ($E_c = 2 \text{ GPa}$, density $\rho_c = 1.56 \text{ Mg m}^{-3}$). This demonstrates that such a structure can be simultaneously stiffer, lighter and thinner than a monolithic aluminium sheet. The comparison with experimental results shown in Fig.2(b) indicated that the flocked sheet has only about 50% of the predicted stiffness, while the figure for the short fibre 3-D array sheet is about 70%. This is attributed to poor resistance offered by the flocked core structure to in-plane shear and lateral compression.

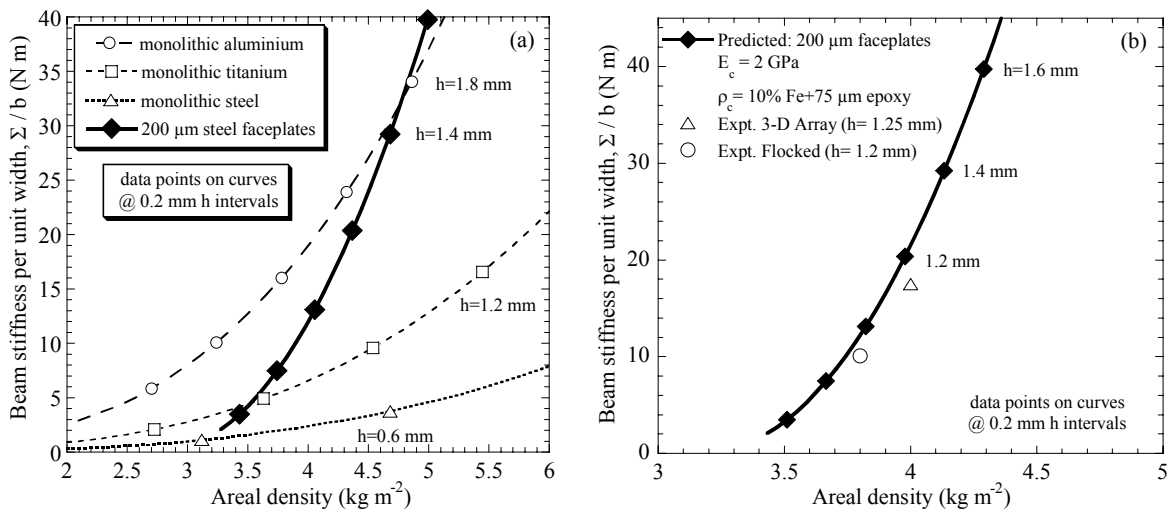


Fig.2: Beam stiffness as a function of areal density, showing (a) benefits of a sandwich structure (isotropic core with $E_c = 2 \text{ GPa}$, $\rho_c = 1.56 \text{ Mg m}^{-3}$) and (b) comparison between theory and experiment.

Through-thickness core stiffness

Two different approaches, based on a cantilever bending model, have been used to predict the through-thickness stiffness of the sandwich sheet cores. The first is applicable for the flocked sheet, in which the fibres are inclined at a specified angle, whereas the second approach assumes a three-dimensionally random orientation distribution of the fibre axes (short fibre 3-D array sheet).

Flocked sheet

The Young's modulus of the core in the through-thickness direction can be predicted by considering the behaviour of a single fibre of length L , initially straight and inclined at an angle θ to the direction of the applied load. The situation under load is depicted schematically in Fig.3. All fibres inclined at such an angle will behave similarly under the action of an imposed load W normal to the plane of the sheet, provided any interaction between individual fibres is neglected and assuming that their behaviour remains linearly elastic. From elementary beam bending theory, the normal deflection, δ ($=\Delta z/\sin\theta$), of the free end of a cantilever beam of length $L/2$, subjected to a load $W\sin\theta$ normal to the beam axis, is given by

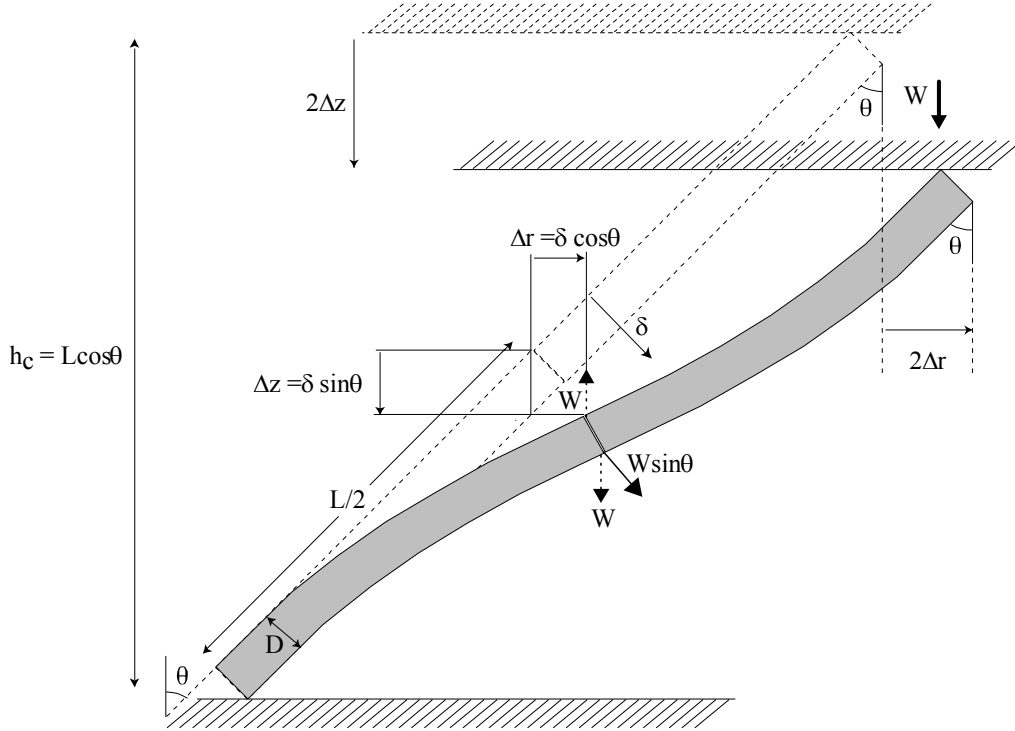


Fig.3: Elevation view of the elastic bending of an inclined fibre under the influence of a vertical load, W .

$$\frac{\Delta z}{\sin\theta} = \frac{1}{3} \frac{W \sin\theta (L/2)^3}{E_f I} \quad (1)$$

where E_f is the fibre modulus and I is the moment of inertia of the fibre section ($=\pi D^4/64$, where D is the fibre diameter, for cylindrical fibres).

The through-thickness strain of the core, ϵ_c , is given by

$$\epsilon_c = \frac{2\Delta z}{h_c} \quad (2)$$

Substituting for Δz from eqn.(1), and writing the core thickness as $L\cos\theta$ (see Fig.3), leads to

$$\epsilon_c = \frac{2W \sin^2\theta (L/2)^3}{3E_f (\pi D^4/64) L\cos\theta} = \frac{16W \sin^2\theta L^2}{3E_f \pi D^4 \cos\theta} \quad (3)$$

Now, the applied pressure, P , can be expressed in terms of the value of W and the number of fibres per unit area, N

$$P = NW \quad (4)$$

There is a relationship between N and the fibre volume fraction, f , which can be expressed as the ratio between the volume occupied by fibres in unit area of core and the corresponding volume of core

$$N = \frac{4f \cos\theta}{\pi D^2} \quad (5)$$

Substituting for N from eqn.(5), the Young's modulus of the core in the through-thickness direction can be expressed as

$$E_c = \frac{P}{\epsilon_c} = \frac{3NW E_f \pi D^4 \cos\theta}{16W \sin^2\theta L^2} = \frac{3(4f\cos\theta) E_f \pi D^4 \cos\theta}{16(\pi D^2) \sin^2\theta L^2} = \frac{3E_f f}{4s^2 \tan^2\theta} \quad (6)$$

where $s (=L/D)$ is the fibre aspect ratio.

Predictions[†] obtained using eqn.(6) show that higher stiffness is predicted for fibres inclined at low angles, as expected, since a fibre provides less resistance to vertical displacement when it is inclined at a high angle. It may also be noted that, for a given volume fraction of fibre, there will be more fibres per unit area when θ is close to 0° (see eqn.(5)). Also, the fibres will be of lower aspect ratio, for a given core thickness. The net effect is cumulative, so the sensitivity of the stiffness to θ is quite strong ($\tan^2\theta$). Furthermore, it can be seen that the stiffness goes up sharply as the fibre aspect ratio is decreased. An obvious way of increasing the stiffness, for a given core thickness, is to use fibres with larger diameter. An increase in fibre content will also generate increased stiffness, but this is less efficient and, of course, it also raises the density of the core.

3-D Random Fibre Array

The cantilever bending model (Fig.3) can be also used to predict the elastic stiffness of an isotropic random fibre array. In this case, the fibre being considered does not span the two faceplates, but is just a segment between two fibre-fibre joints (see Fig.1(b)). The deflection is induced by an applied stress, σ (compressive in Fig.3), which generates a force W on each individual fibre segment. These are related by

$$\sigma = NW \quad (7)$$

where N is the number of fibre segments per unit sectional area.

For a 3-D random fibre array, the relationship between N and f is simply obtained by noting that, for a set of prisms with a 3-D random orientation distribution of the prism axes, the area intersected by any plane is twice the area intersected by a plane lying normal to the alignment direction of a set of parallel prisms occupying the same volume fraction[10]. Hence, N here has a value of half that for the case of an aligned set of cylinders ($=f/(\pi D^2/4)$), ie

$$N = \frac{2f}{\pi D^2} \quad (8)$$

As before, the normal deflection, δ , of the end of a cantilever beam of length $L/2$, subjected to a load $W \sin\theta$ normal to the beam axis, is given by

$$\delta = \frac{W \sin\theta (L/2)^3}{3E_f \left(\frac{\pi D^4}{64}\right)} = \frac{8W \sin\theta L^3}{3E_f \pi D^4} \quad (9)$$

so that, substituting for W from eqns.(7) and (9) and N from eqn.(8), the axial deflection is given by

$$\Delta z = \delta \sin\theta = \frac{4\sigma L^3 \sin^2\theta}{3E_f f D^2} \quad (10)$$

The overall deformation expected with a material composed of a three-dimensionally random array of fibres can be analysed, at least approximately, by summing the contributions[§] from individual fibre segment deformations. The segments are assumed to exhibit a spherically symmetric orientation distribution, which has a $\sin\theta$ angular probability distribution about any given axis. The expected overall relative net extension in the direction of an applied stress can therefore be written down by considering the displacements of a set of fibre mid-points, using the expression for the deflection normal to the fibre axis, as a function of the distance

[†] This treatment clearly breaks down in the limit of $\theta=0^\circ$, when the predicted stiffness tends to infinity. The value must be upper bounded at fE_f , corresponding to the fibres remaining vertical and being axially compressed. In practice, even this value would not be approached, at least for fibres with relatively high aspect ratios. Realistically, the model may be taken as applicable for angles down to around $5-10^\circ$, which is probably all that is required.

[§] In reality, the deflections exhibited by individual fibre segments will be influenced by the configuration of neighbouring segments, so this analysis is clearly not rigorous when the inclination angles vary within the material. For example, the axial deflection of a segment inclined at a substantial angle to the stress axis would be reduced if a closely neighbouring segment were aligned parallel to the axis. However, such interactions are unlikely to generate large errors in the proposed model, at least for an effectively isotropic, homogeneous material.

along the fibre, given by eqn.(10). The macroscopic deflection in the loading direction, and hence the strain, can thus be expressed as

$$\varepsilon_c = \frac{\Delta Z}{Z} = \frac{\int_0^{\pi/2} \Delta z \sin \theta d\theta}{\int_0^{\pi/2} z \sin \theta d\theta} = \frac{\int_0^{\pi/2} \frac{4\sigma L^3 \sin^3 \theta}{3E_f f D^2} d\theta}{\int_0^{\pi/2} \left(\frac{L}{2} \cos \theta\right) \sin \theta d\theta}$$

$$\therefore \varepsilon_c = \left(\frac{8\sigma}{3E_f f}\right) \left(\frac{L}{D}\right)^2 \frac{\int_0^{\pi/2} \sin^3 \theta d\theta}{\int_0^{\pi/2} \cos \theta \sin \theta d\theta} = \left(\frac{32\sigma}{9E_f f}\right) \left(\frac{L}{D}\right)^2 \quad (11)$$

The Young's modulus of the fibre array, $E_c (= \sigma/\varepsilon)$, is therefore given by

$$\therefore E_c = \frac{9E_f f}{32 \left(\frac{L}{D}\right)^2} = \frac{9E_f f}{32 s^2} \quad (12)$$

A comparison between experimental results and predictions obtained using eqn.(6) (flocked sheet) and eqn.(12) (short fibre 3-D array sheet) is shown in Fig.4. It can be seen that experimental data are broadly consistent with predictions from the model predictions. For the flocked sheet, the measured value of about 100 MPa is in fairly good agreement with predictions obtained using estimated values for s , f and θ of 33 ($= h_c / D \sin \theta$), 8% and 15° respectively. For the short fibre 3-D array, the measured value of about 100 MPa is in fairly good agreement with predictions obtained using estimated values for s and f of 6 and 10% respectively. In any event, it is clear that all of these stiffnesses are relatively low (appreciably lower, for example, than would be the case if the cavity were filled with resin, ie $\sim 1-3$ GPa), and that these results are broadly consistent with the model predictions.

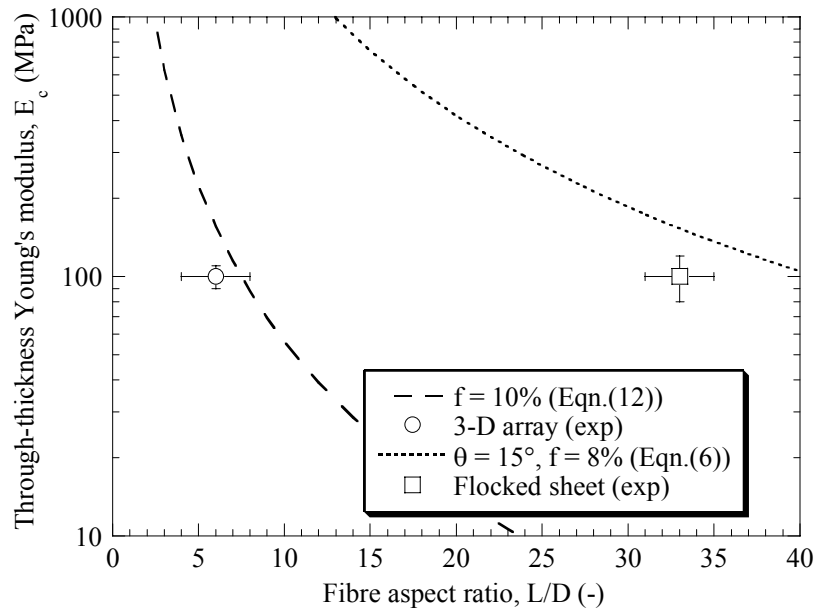


Fig.4: Through-thickness Young's modulus of the core as a function of fibre aspect ratio. The two points correspond to experimental measurements, while the curves are predictions obtained using eqns.(6) and (12). A value of 200 GPa was used for the stiffness of the stainless steel fibres.

Conclusions

The following conclusions can be drawn from this work.

- (a) Two variants of a novel, thin sandwich steel sheet, with a steel fibre core, have been characterised in terms of core structure. One variant (flocked sheet) contains strong fibres oriented approximately normal to the plane of the sheet and bonded to the faceplates by adhesive. The second variant (short fibre 3-D array) contains an approximately 3-D random network of coarser fibres, brazed to each other and to the faceplates.
- (b) The beam stiffnesses of these sheets have been measured and the results compared with values expected from conventional bending theory, assuming the core to be isotropic. In both cases, the measured stiffnesses were lower than predicted. The measured through-thickness Young's moduli are relatively low (~100 MPa) and are broadly consistent with predictions from an analytical model based on the bending of individual fibres. In this context, it is worth noting that, in sandwich sheets, the bending stiffness is dominated by the faceplates, so the core does not necessarily need to be very stiff. However, very compliant cores might be problematic, in that they may allow excessive shear between the faceplates or failure to maintain faceplate separation under load, leading to low beam stiffness. The brazed 3-D random fibre array core performs appreciably better than the flocked sheet core in this regard.

Acknowledgements

Support for this work is being provided by the Cambridge-MIT Institute (CMI). The authors wish to acknowledge Mr. Andrew Cockburn, of Cambridge University, who made some of the stiffness measurements and produced the 3-D array sheet., Mr. Jerry Karlsson, of HSSA Ltd, for providing the flocked sheet and Peter Rooney and Lee Marston, of FibreTech, for supplying the fibres.

References

1. T.M. McCormack, R. Miller, O. Kesler and L.J. Gibson, "Failure of Sandwich Beams with Metallic Foam Cores", *Int. J. of Solids and Structures*, 38, 4901-4920 (2001).
2. C. Chen, A.M. Harte and N.A. Fleck, "The Plastic Collapse of Sandwich Beams with a Metallic Foam Core", *Int. J. Mech. Sci.*, 43, 1483-1506 (2001).
3. A.M. Harte, N.A. Fleck and M.F. Ashby, "Sandwich Panel Design using Aluminium Alloy Foam", *Adv. Engng. Mater.*, 2, 219-222 (2000).
4. T.S. Lok and Q.H. Chen, "Elastic Stiffness Properties and Behavior of Truss-Core Sandwich Panel", *J. Structural Engineering - ASCE*, 126, 552-559 (2000).
5. D.J. Sypeck and H.N.G. Wadley, "Multifunctional Microtruss Laminates: Textile Synthesis and Properties", *J. Mater. Res.*, 16, 890-897 (2001).
6. S. Chiras, D.R. Mumm, A.G. Evans, N. Wicks, J.W. Hutchinson, K. Dharmasena, H.N.G. Wadley and S. Fichter, "The Structural Performance of Near-Optimized Truss Core Panels", *Int. J. of Solids and Structures*, 39, 4093-4115 (2002).
7. R. Gustavsson, "Formable Sandwich Construction Material and Use of the Material as Construction Material in Vehicles, Refrigerators, Boats etc", patent WO 98/01295, AB Volvo, International (1998).
8. A.E. Markaki and T.W. Clyne, "Mechanics of Thin Ultra-Light Stainless Steel Sandwich Sheet Material: Part I - Stiffness", *Acta Mater.*, 51, 1341-1350 (2003).
9. A.E. Markaki and T.W. Clyne, "Mechanics of Thin Ultra-Light Stainless Steel Sandwich Sheet Material: Part II - Resistance to Delamination", *Acta Mater.*, 51, 1351-1357 (2003).
10. E.E. Underwood, *Quantitative Stereology*, Reading: Addison-Wesley Publishing Company (1970).